

# IBA57 Recruits ISCA2 to Form a [2Fe-2S] Cluster-Mediated Complex

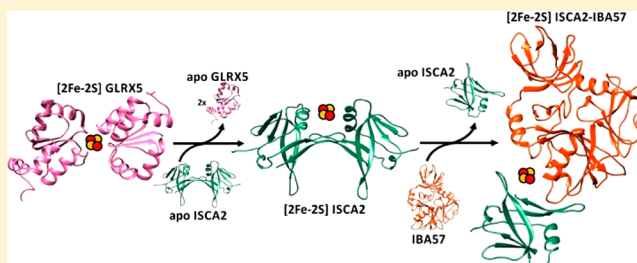
Spyridon Gourdoups,<sup>†,§</sup> Veronica Nasta,<sup>†,‡,§</sup> Vito Calderone,<sup>†,‡,§</sup> Simone Ciofi-Baffoni,<sup>\*,†,‡,§</sup> and Lucia Banci<sup>\*,†,‡,§</sup>

<sup>†</sup>Magnetic Resonance Center CERM, University of Florence, Via Luigi Sacconi 6, 50019 Sesto Fiorentino, Florence, Italy

<sup>‡</sup>Department of Chemistry, University of Florence, Via della Lastruccia 3, 50019 Sesto Fiorentino, Florence, Italy

## Supporting Information

**ABSTRACT:** The maturation of mitochondrial iron-sulfur proteins requires a complex protein machinery. Human IBA57 protein was proposed to act in a late phase of this machinery, along with GLRX5, ISCA1, and ISCA2. However, a molecular picture on how these proteins cooperate is not defined yet. We show here that IBA57 forms a heterodimeric complex with ISCA2 by bridging a [2Fe-2S] cluster, that [2Fe-2S] cluster binding is absolutely required to promote the complex formation, and that the cysteine of the conserved motif characterizing IBA57 protein family and the three conserved cysteines of the ISCA protein family act as cluster ligands. The [2Fe-2S] heterodimeric complex is the final product when IBA57 is either exposed to [2Fe-2S] ISCA2 or in the presence of [2Fe-2S] GLRX5 and apo ISCA2. We also find that the [2Fe-2S] ISCA2-IBA57 complex is resistant to highly oxidative environments and is capable of reactivating apo aconitase *in vitro*. Collectively, our data delineate a [2Fe-2S] cluster transfer pathway involving three partner proteins of the mitochondrial ISC machinery, that is, GLRX5, ISCA2 and IBA57, which leads to the formation of a [2Fe-2S] ISCA2-IBA57 complex.



## INTRODUCTION

The biogenesis of iron-sulfur (Fe-S) proteins in humans is a multistage process occurring in different cellular compartments.<sup>1–4</sup> In mitochondria, this process is accomplished by the so-called iron-sulfur cluster (ISC) assembly machinery.<sup>5</sup> Members of the mitochondrial ISC assembly machinery include the A-type ISC proteins and monothiol glutaredoxins.<sup>6–10</sup> The human genome encodes two A-type ISC proteins, termed ISCA1 and ISCA2, which are functionally related to the *Saccharomyces cerevisiae* Isa1 and Isa2.<sup>11</sup> The latter were shown to be specifically required for the maturation of mitochondrial [4Fe-4S] proteins.<sup>12,13</sup> In yeast, Isa1 and Isa2 interact with monothiol glutaredoxin-5, the protein receiving a *de novo* assembled [2Fe-2S] cluster from a scaffold protein of the mitochondrial ISC assembly machinery.<sup>9,14</sup> Isa1 and Isa2 form a heterocomplex, and both interact with Iba57, another mitochondrial protein of the ISC assembly machinery which contains a highly conserved motif, KGC(Y/F)XGQE, that characterizes a protein family (PTHR22602 and COG0354) of unknown biochemical function, widely represented across eubacterial and eukaryotic taxa, including humans.<sup>12,15–17</sup> Deletions of either yeast *ISA1*, *ISA2*, or *IBA57* genes elicit identical phenotypes, with yeast cells lacking a functional respiratory chain, functional mitochondrial aconitase proteins, and lipoic acid.<sup>12,15</sup> Based on all these data, it has been proposed that the three yeast proteins might act in the same biochemical process by forming a complex.<sup>5</sup> Specifically, it has been suggested that a hetero-oligomeric complex formed by Isa1, Isa2, and Iba57 is the functional unit in *S. cerevisiae*

specifically devoted to convert two [2Fe-2S] clusters to a [4Fe-4S] cluster. This model has been proposed to hold also in humans<sup>18</sup> on the basis of the following experimental data: (i) the maturation of mitochondrial [4Fe-4S] proteins, including aconitase, respiratory complex I, succinate dehydrogenase, and lipoic acid synthase, was impaired upon depletion of each of the three human proteins, similarly to what it occurs in yeast;<sup>11</sup> (ii) the human IBA57 complements the yeast *iba57Δ* growth defects, demonstrating its conserved function throughout the eukaryotic kingdom.<sup>15</sup>

Recent data, however, outlined new possible views on how these three proteins can work in the mitochondrial ISC assembly machinery. Surprisingly, recent knockdown experiments in mouse skeletal muscle and in primary cultures of neurons indicated that ISCA1, and not ISCA2 and IBA57, is required for mitochondrial [4Fe-4S] proteins biogenesis.<sup>19</sup> Moreover, although ISCA1 and ISCA2 reciprocally interact both *in vivo* and *in vitro*,<sup>19,20</sup> only ISCA2 interacts with IBA57 at variance of what was observed in yeast.<sup>19</sup> These results suggested that human ISCA1, ISCA2, and IBA57 do not necessarily act as a ternary complex as proposed for the yeast homologues, but they might modulate their interactions network in a complex and dynamic manner, possibly depending on the physiological state of human cells, tissue, and temporal specificity.<sup>19</sup> Other data supporting the formation of a specific complex between ISCA2 and IBA57

Received: August 22, 2018

Published: October 1, 2018

and not with ISCA1 originate from *in vivo* expression level studies. Specifically, patients with pathogenic IBA57 mutations that markedly reduce the protein levels of IBA57 in fibroblasts mitochondria displayed expression levels of ISCA1 in normal range or slightly overexpressed, while the ISCA2 expression levels were found drastically decreased in all patients.<sup>21</sup> These results are in line with studies performed in HeLa cells where the silencing of IBA57 was associated with unchanged or increased expression of ISCA1.<sup>11</sup> It has also been shown by us through *in vitro* biochemical studies that a heterocomplex between ISCA1 and ISCA2 acts as a platform to assemble a [4Fe-4S] cluster from two [2Fe-2S] clusters donated by dimeric human glutaredoxin GLRX5, without any requirements of IBA57.<sup>20,22,23</sup> These data thus support the model that multiple pathways might be operative for ISCA1, ISCA2, and IBA57.<sup>19</sup> Collectively, the available functional and biochemical data do not allow yet to define a molecular picture on how the ISCA1, ISCA2, and IBA57 proteins cooperate in the mitochondrial ISC assembly machinery, but only suggest that cellular processes with different involvement of ISCA1, ISCA2, and IBA57 might exist. To get further insights on the function of these partner proteins, we have here characterized the interactions among GLRX5, ISCA1, ISCA2, and IBA57 via complementary biophysical techniques. Our results delineate a cluster transfer pathway involving GLRX5, ISCA2 and IBA57, which ends in the formation of a [2Fe-2S] cluster-mediated ISCA2-IBA57 complex, which is resistant to a highly oxidative environment and able to reactivate apo aconitase.

## ■ EXPERIMENTAL SECTION

**Cloning and Mutagenesis.** The gene of human IBA57 (lacking the mitochondrial targeting sequence of 30 amino acids) was made available and inserted in the *EcoRI*-*Sall* cloning site (MCS1) of a pETDuet-1 vector having a N-terminal His-tag at MCS1 site by Twin Helix Srl company. Cys 230 to Ala substitution in IBA57 was obtained by site-directed mutagenesis (QuickChange Site-directed Mutagenesis Kit, Agilent Technologies) applied on the pETDuet-1 vector containing the IBA57 gene.

**Protein Expression and Purification.** The pETDuet-1 plasmid containing N-terminal His-tag IBA57 was transformed in *Escherichia coli* BL21-Gold(DE3) (Agilent) competent cells. Cells were cultivated overnight (O/N) at 37 °C in Luria-Bertani (LB) media adding ampicillin (100 µg/mL) and 3% of ethanol per liter of sterile LB. The following day the cells were spun down (3000 rpm for 20 min) and resuspended in 1 L of fresh LB or minimal media [with 1 g (<sup>15</sup>NH<sub>4</sub>)<sub>2</sub>SO<sub>4</sub> and 3 g glucose] containing ampicillin (100 µg/mL) and 3% of ethanol. The culture was left at 37 °C, 160 rpm for approximately 1 h, and then a heat shock procedure [10 min at 42 °C (160 rpm), 20 min at 37 °C (160 rpm), 30 min in ice and 20 min at 37 °C (160 rpm)] was performed on the culture to induce a high level of heat shock *E. coli* proteins, in order to allow effective enhancement of the solubility and thereby the yield of overexpressed protein in *E. coli*.<sup>24</sup> Protein expression was then induced by adding 0.1 mM of isopropyl β-D-1-thiogalactopyranoside (IPTG), shaking O/N at 18–20 °C (160 rpm).

The cell paste was dissolved in the binding buffer (50 mM phosphate buffer, 500 mM NaCl, 20 mM imidazole, pH 7.6), and after sonication, the N-terminal His-tag IBA57 protein was purified from *E. coli* using a HisTrap HP column (GE Healthcare). The His-tag was cleaved by tobacco etch virus protease (1 mg) O/N at room temperature in 50 mM phosphate buffer, 500 mM NaCl, 500 mM imidazole, pH 7.6. A second His-trap chromatography column on the latter mixture was performed to separate digested IBA57 from His-tag IBA57. Recovered IBA57 was pure enough to be used for spectroscopic and biochemical studies. To obtain a highly purified sample for crystallization trials, a size exclusion chromatography using

a HiLoad 16/60 Superdex™ 75 pg column, attached to an ÄKTA pure chromatography unit, was performed. The final yield was about 14 mg per liter of culture. 2.5 mM tris (2-carboxyethyl) phosphine (TCEP) was added in all the purification steps to avoid disulfide bond formation. The same procedure was followed to produce the Cys230Ala IBA57 mutant, wherein the yield was about 21 mg per liter of culture.

The expression and purification of wild-type apo- and holo- ISCA1, ISCA2, and GLRX5 proteins and of Cys79Ser, Cys144Ser, and Cys146Ser ISCA2 mutants were obtained as already reported.<sup>20,22,23</sup>

Apo ISCA1 and 1:1 (referring to monomeric protein concentrations) protein mixtures of apo ISCA1-IBA57, apo ISCA2-IBA57 (or Cys230Ala IBA57), and apo Cys79Ser or Cys144Ser or Cys146Ser ISCA2-IBA57 were chemically reconstituted in anaerobic conditions in 50 mM Tris-HCl, 100 mM NaCl, 5 mM DTT buffer at pH 8.0 with three-fold FeCl<sub>3</sub> and Na<sub>2</sub>S for 16 h at room temperature. Chemical reconstitution was performed with protein concentration range from 30 to 50 µM. The [2Fe-2S] cluster-bound form of ISCA2 was obtained by anaerobic chemical reconstitution in the same conditions as above but with stoichiometric FeCl<sub>3</sub> and Na<sub>2</sub>S for 16 h at room temperature. The latter procedure produced a mixture of apo and [2Fe-2S] cluster bound ISCA2 in ratios ranging from 30:70 to 40:60.

Cytosolic aconitase was expressed and purified by using pT7-his-hIRP1 plasmid, kindly provided by Prof. Matthias W. Hentze, European Molecular Biology Laboratory (EMBL), Heidelberg, Germany. The production and chemical reconstitution of aconitase was obtained following a previously reported protocol.<sup>25</sup>

**Spectroscopic, Biophysical, and Activity Analysis.** UV–vis and CD spectra were acquired at 20 °C, aerobically or anaerobically in degassed buffer (50 mM phosphate buffer, 150 mM NaCl, 5 mM DTT, pH 7.0) on a Cary 50 Eclipse spectrophotometer and JASCO J-810 spectropolarimeter, respectively.

SEC-MALS data were acquired by attaching a Superdex™ 200 Increase 10/300 GL column to a DAWN HELEOS system with a continuous flow rate of 0.6 mL/min using a filtered buffer (50 mM phosphate buffer, 150 mM NaCl, pH 7.0). Analytical gel filtration was performed by attaching a Superdex™ 200 Increase 10/300 GL column to an ÄKTA pure chromatography unit with a flow rate of 0.75 mL/min using a buffer consisting of 50 mM phosphate buffer, 150 mM NaCl, pH 7.0.

Aerobically purified cytosolic aconitase (5 µM) was incubated at 25 °C for 45 min with the five-fold excess of [2Fe-2S] ISCA2-IBA57 complex in 50 mM phosphate buffer, 150 mM NaCl, 5 mM DTT, pH 7.0. The reaction was then followed by measuring aconitase activity. The aconitase activity was assayed by the Aconitase Activity Assay kit (Sigma-Aldrich MAK051) as described in Maione et al.<sup>25</sup>

**AMS-Based Alkylation Gel Shift Assay.** A gel shift assay on samples previously modified with 4-acetamido-4-maleimidylstilbene-2,2-disulfonic acid (AMS) was performed.<sup>26</sup> For this purpose, IBA57, Cys230Ala IBA57, and the [2Fe-2S] ISCA2-IBA57 were incubated with 10 mM AMS in 50 mM phosphate buffer, pH 7.0, 150 mM NaCl for 30 min at 25 °C. Samples were then precipitated with 10% trichloroacetic acid. Pellets were washed with acetone and resuspended in 80 mM Tris-HCl, pH 6.8, 8 M urea. Samples were separated by nonreducing SDS-PAGE, and the gel was stained with Coomassie Blue. AMS reacts with available thiol groups, resulting in a mobility shift of the protein on SDS-PAGE due to its increase in size of 0.5 kDa per added molecule AMS.

**X-ray Crystallography.** Crystals of wild-type and Cys203Ala IBA57 were grown by the sitting-drop vapor diffusion method at 25 °C by mixing equal volumes (2 µL) of the protein solution and the reservoir solution. The protein concentration range was 0.2–0.4 mM, in 50 mM phosphate buffer, 150 mM NaCl, and 2.5 mM TCEP, pH 7.0. The reservoir solution used for both consisted of 20% (w/v) PEG 3350 and 200 mM NaCl. In the case of wild-type IBA57 crystals, a reservoir solution consisting of 20% (w/v) PEG 3350 and 200 mM NaCl and 100 mM MES pH 6.0 was also used. The structure determination has been carried out through anomalous dispersion.

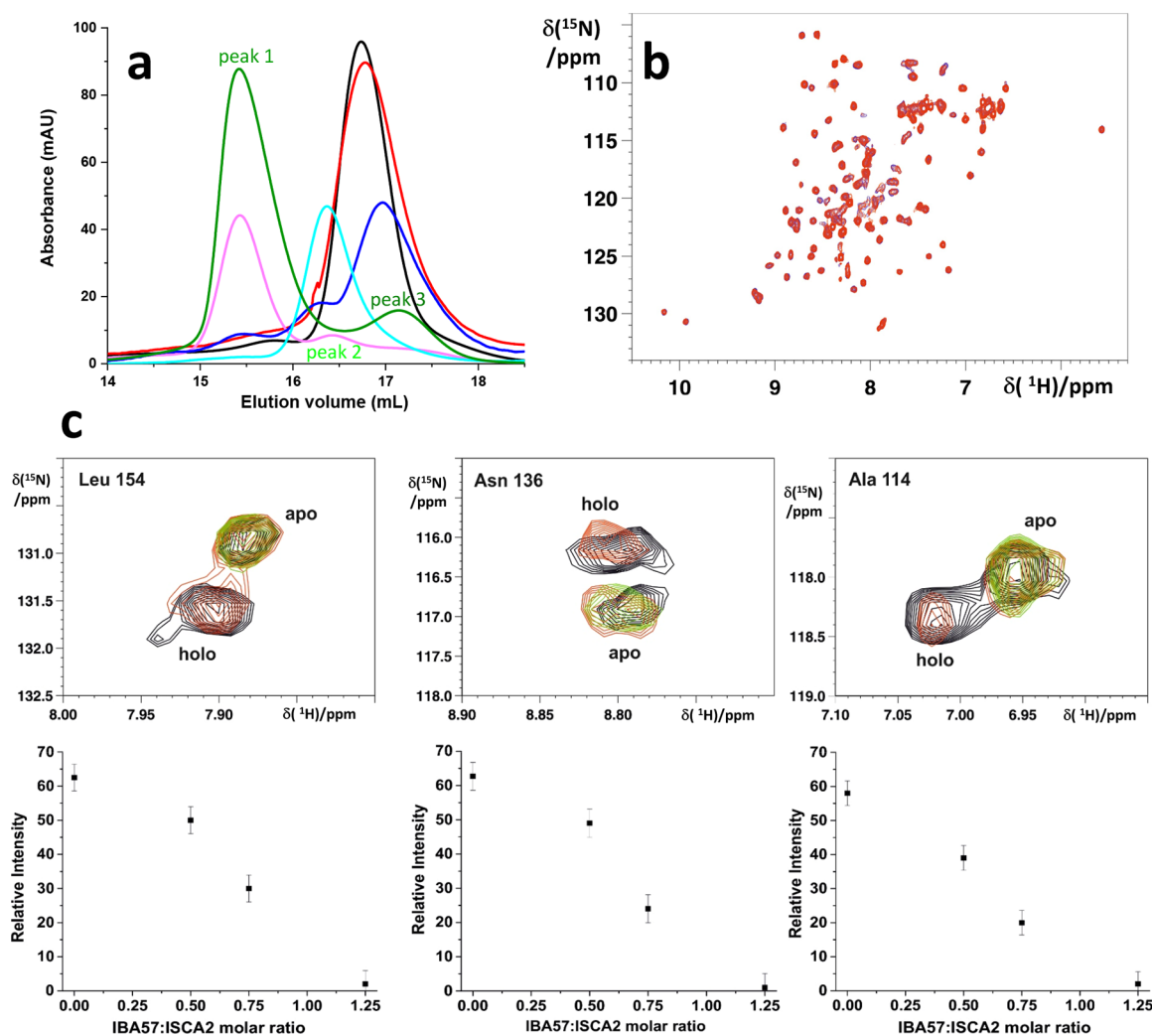


**Figure 1.** Complex formation between [2Fe-2S] ISCA2 and IBA57. (a) Elution profiles obtained for IBA57 (black), apo ISCA2 (blue), [2Fe-2S] ISCA2 (cyan), a 1:1 mixture of IBA57 and apo ISCA2 (red), a 1:0.5 and 1:1 (these two ISCA2:IBA57 ratios based on dimeric [2Fe-2S] ISCA2 concentration vs monomeric IBA57 concentration) mixture of IBA57 and [2Fe-2S]/apo ISCA2 (magenta and dark green, respectively) by gel filtration on analytical Superdex<sup>TM</sup> 200 Increase 10/300 GL column. mAU: milli absorbance unit. (b) Overlay of  $^1\text{H}$ - $^{15}\text{N}$  HSQC spectra of  $^{15}\text{N}$ -labeled apo ISCA2 (0.7 mM) in the absence (blue) and in the presence (red) of 1 equiv of IBA57. (c) In the upper panels,  $^1\text{H}$ - $^{15}\text{N}$  HSQC spectral regions for three residues of  $^{15}\text{N}$ -labeled [2Fe-2S]/apo ISCA2 (0.6 mM: 0.35 mM [2Fe-2S] ISCA2 and 0.25 mM apo ISCA2) with the apo and the holo forms in slow exchange on the NMR time scale are shown in the absence (black) and in the presence of 0.5 equiv (red) and 1 equiv (green) of IBA57 relative to [2Fe-2S] ISCA2 concentration. In the lower panels, the relative intensity of the backbone amide signals of these three residues for the holo species is plotted against the IBA57:ISCA2 ratio. Data are represented as the mean of three measurements  $\pm$  s.d.

**EPR and NMR Spectroscopy.** EPR spectra of the [2Fe-2S] ISCA2-IBA57 complex (400  $\mu\text{M}$ ) were recorded before and after anaerobic reduction of the cluster by addition of sodium dithionite and rapid freezing of the protein solution in liquid nitrogen. EPR spectra were recorded in degassed 50 mM phosphate buffer, 150 mM NaCl, 5 mM DTT, pH 7.0, and 10% (v/v) glycerol at 45 K or 5 K, using a Bruker Elexsys E500 spectrometer working at a microwave frequency of ca. 9.39 GHz, equipped with a SHQ cavity and a continuous cryostat He flow (ESR900, Oxford instruments) for temperature control. Acquisition parameters were as follows: microwave power 5 mW; modulation frequency 100 kHz; modulation amplitude 8.0 G; acquisition time constant 163.84 ms; number of points 1024.

NMR experiments were recorded on Bruker AVANCE 400, 700, 900, and 950 MHz spectrometers at 298 K on 0.3–1 mM protein samples, in 50 mM phosphate buffer, 5 mM DTT, and 150 mM NaCl, pH 7.0, and 10% (v/v)  $\text{D}_2\text{O}$ . Spectra were processed using TopSpin (Bruker BioSpin) and analyzed with CARA software. The interaction between [2Fe-2S]/apo ISCA2 and IBA57 was followed by  $^1\text{H}$ - $^{15}\text{N}$  HSQC NMR spectra titrating  $^{15}\text{N}$ -labeled apo/[2Fe-2S] ISCA2 with

unlabeled apo IBA57 up to a 1:1 protein ratio (ISCA2:IBA57 protein ratio based on dimeric [2Fe-2S] ISCA2 concentration vs monomeric IBA57 concentration). Cluster transfer from homodimeric [2Fe-2S] GLRX5 to apo ISCA2/IBA57 mixture was followed by  $^1\text{H}$ - $^{15}\text{N}$  HSQC NMR spectra titrating a 1:1 mixture of  $^{15}\text{N}$ -labeled apo ISCA2 and unlabeled IBA57 up to a final 1:1:2 ratio referring to monomeric protein concentrations. NMR titrations were successfully repeated three times in all cases.

1D  $^1\text{H}$  paramagnetic-tailored NMR experiments were performed at 400 MHz with a  $^1\text{H}$  optimized 5 mm probe. Water signal was suppressed via fast repetition experiments and water selective irradiation. Experiments were typically performed using an acquisition time of 50 ms and an overall recycle delay of 90 ms. The heterocomplex concentration was 0.5 mM. Squared cosine and exponential multiplications were applied prior to Fourier transformation. Manual baseline correction was performed, using polynomial functions.

The interaction of IBA57 with tetrahydrofolic acid (THF) and the calcium salt of folinic acid (calcium folinate) was followed, respectively, by  $^1\text{H}$ - $^{15}\text{N}$  HSQC NMR titration experiments at 298

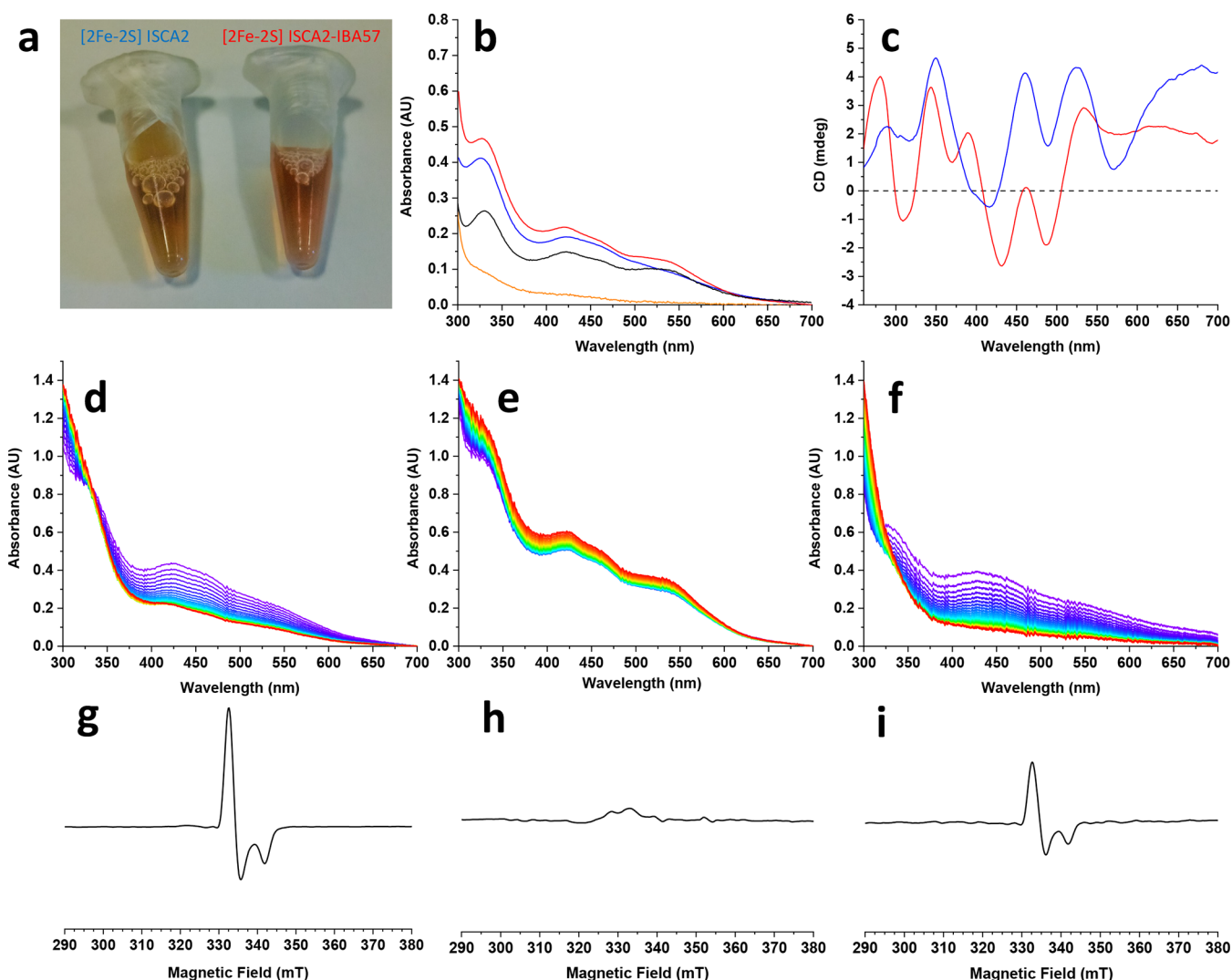


**Figure 2.** The ISCA2-IBA57 complex binds a [2Fe-2S] cluster as observed by UV-vis, CD, and EPR spectroscopies. (a) Pictures of [2Fe-2S]/apo ISCA2 before (on the left) and after (on the right) the addition of 1 equiv of IBA57 with respect to dimeric [2Fe-2S] ISCA2 concentration. (b) UV-vis spectra of [2Fe-2S]/apo ISCA2 (blue), of a 1:1 mixture of IBA57 and [2Fe-2S]/apo ISCA2 (red), of peak 1 fractions obtained by gel filtrating the 1:1 [2Fe-2S]/apo ISCA2-IBA57 mixture (black), and of peak 3 fractions obtained by gel filtrating the 1:1 [2Fe-2S]/apo ISCA2-IBA57 mixture (orange). AU: absorbance unit. (c) CD spectra of [2Fe-2S]/apo ISCA2 (blue), of a 1:1 mixture of IBA57 and [2Fe-2S]/apo ISCA2 (red). UV-vis spectra of (d) [2Fe-2S]/apo ISCA2, (e) of a 1:1 mixture of IBA57 and [2Fe-2S]/apo ISCA2, and (f) of the chemically reconstituted 1:1 ISCA2-Cys230Ala IBA57 mixture, collected upon air exposure every 30 min for 15 h. The colors of the traces follow visible spectrum trend from violet (starting point) to final point (red). X-band EPR spectra of the 1:1 mixture of IBA57 and [2Fe-2S]/apo ISCA2 at 45 K before (g) and after (h) being exposed overnight in air and (i) upon addition of two equivalents of dithionite. The experiments were conducted with protein concentration of dimeric ISCA2 ranging from 0.075 mM to 0.3 mM depending on the applied spectroscopic technique.

K and by  $^1\text{H}$  1D enhanced Protein Hydration Observed by Gradient Spectroscopy (ePHOGSY) NMR experiments at 298 K.<sup>27</sup> The sample for the  $^1\text{H}$ - $^{15}\text{N}$  HSQC NMR experiments was 0.35 mM in  $^{15}\text{N}$ -labeled IBA57 final concentration and 0.7 mM in THF final concentration. Samples of ePHOGSY experiments were 10  $\mu\text{M}$  in IBA57 concentration and 5 mM in calcium folinate concentration, in 50 mM phosphate buffer, 150 mM NaCl, 10%  $\text{D}_2\text{O}$ , and trimethylsilylpropanoic acid as an internal standard. NMR experiments to follow the interaction of tetrahydrofolate derivatives with IBA57 were repeated twice. ePHOGSY NMR experiments were also performed on the [2Fe-2S] ISCA2-IBA57 heterocomplex (10  $\mu\text{M}$ ) in the presence of 1 mM calcium folinate.

**Data Availability.** Coordinates and structure factors of IBA57 and Cys230Ala IBA57 have been deposited under accession codes 6ESR and 6GEU, respectively.

## RESULTS

**IBA57 Forms a Complex with ISCA2 upon [2Fe-2S] Cluster Binding.** Analytical gel filtration equipped with multiangle light scattering (SEC-MALS) showed that IBA57 elutes as a single peak with a molar mass of  $37.4 \pm 0.5$  kDa (Figure 1a and Figure S1), which is close to the molecular weight calculated from the cloned amino acid sequence (34925 Da). The protein is unable to bind a Fe-S cluster, either through various chemical reconstitution procedures or when produced by cells supplemented with excess of iron ions. Furthermore, IBA57 is unable to receive a [2Fe-2S] cluster from human monothiol glutaredoxin-5 (GLRX5), which typically donates [2Fe-2S] clusters to several possible acceptors.<sup>23,28,29</sup> These data indicate that the protein is monomeric and cannot bind a Fe-S cluster on its own.

Since human ISCA2 has been found to specifically interact *in vivo* with IBA57,<sup>19</sup> the interaction of IBA57 with both apo and [2Fe-2S]-bound forms of ISCA2 was analyzed *in vitro* by SEC-MALS and NMR. ISCA2 is a dimer in both the apo and the holo forms and can bind a [2Fe-2S] or a [4Fe-4S] cluster at the same binding site, through Cys 79 from the two subunits of the dimer, Cys 144 from one subunit, and Cys 146 from the other subunit.<sup>20,22</sup> When IBA57 is mixed with apo ISCA2, no complex formation occurs between the two proteins. Indeed, SEC-MALS of the protein mixture at 1:1 protein ratio did not show the presence of any peak at elution volumes higher than those of monomeric IBA57 and dimeric apo ISCA2 in any tested condition (Figure 1a). <sup>1</sup>H–<sup>15</sup>N HSQC NMR experiments, performed on <sup>15</sup>N-labeled apo ISCA2 stepwise titrated with unlabeled IBA57 up to a 1:1 protein ratio, did not show any chemical shift variation or line-broadening effect, indicating again that the two proteins do not interact with each other in the absence of a Fe-S cluster bound to ISCA2 (Figure 1b). On the contrary, when IBA57 is added, in anaerobic conditions, to the mixture of apo and [2Fe-2S]<sup>2+</sup> cluster-bound ISCA2, as it is obtained after ISCA2 chemical reconstitution ([2Fe-2S]/apo ISCA2, hereafter, see Experimental Section for details), SEC-MALS showed the formation of a new species eluting with a molar mass of 51.2 ± 0.5 kDa (peak 1 in Figure 1a and Figure S1), which is close to the sum of the molecular weights of a molecule of monomeric ISCA2 (12565 Da) and a molecule of monomeric IBA57 (34925 Da), as calculated from the cloned amino acid sequences. SDS-PAGE performed on the elution fractions of this new species showed that they contain both IBA57 and ISCA2 proteins, according to complex formation between the two proteins (Figure S2). In line with the formation of a heterodimeric ISCA2-IBA57 complex, a minor peak (peak 2 in Figure 1a) with an elution volume of [2Fe-2S] ISCA2 is present when IBA57 is substoichiometrically added to [2Fe-2S]/apo ISCA2, while a minor peak (peak 3 in Figure 1a) with the same elution volume of apo ISCA2 is observed when IBA57 is present at the stoichiometric ratio. <sup>1</sup>H–<sup>15</sup>N HSQC NMR experiments were performed on a <sup>15</sup>N-labeled [2Fe-2S]/apo ISCA2 stepwise titrated with unlabeled IBA57. Line-broadening in the NMR spectra was observed exclusively on the backbone NH cross-peaks of the [2Fe-2S] ISCA2 species, while the line-width of the apo ISCA2 cross-peaks remain unchanged (Figure 1c). The line-broadening effects on the cross-peaks of the [2Fe-2S] ISCA2 species increase with the additions, until some signals disappeared once a final 1:1 protein ratio was reached (Figure 1c). Overall, SEC-MALS and NMR data showed that a subunit of homodimeric [2Fe-2S] ISCA2 is replaced by IBA57 to form a heterodimeric complex and that apo ISCA2, which does not interact with IBA57, is released in solution. These data also demonstrated that cluster binding is required to promote complex formation between ISCA2 and IBA57 proteins. We can therefore define such interaction as cluster mediated.

As a Fe-S cluster is required to induce complex formation, we could deem that IBA57 is involved in Fe-S cluster binding in the complex providing one or more cluster ligand(s). In order to investigate such a possibility, a combination of UV-vis absorption, UV-vis circular dichroism (CD), and EPR spectroscopies has been applied to analyze the nature and properties of the cluster bound to the complex. Upon mixing [2Fe-2S]/apo ISCA2 with IBA57, the UV-vis spectra showed an increase of the band at 540 nm, which is very weak in [2Fe-2S]<sup>2+</sup> ISCA2, with a simultaneous change of the color of the

solution from yellowish-brown to pinkish-red (Figure 2a,b). The UV-vis spectrum of the mixture maintains all the absorption bands of biological oxidized [2Fe-2S]<sup>2+</sup> centers, which typically have bands centered at around 330, 420, 460, and 550 nm, all attributable to S–Fe(III) charge-transfer (CT) transitions (Figure 2b).<sup>30</sup> Also paramagnetic NMR spectroscopy indicates the presence of a bound [2Fe-2S]<sup>2+</sup> cluster. Indeed, the paramagnetic 1D <sup>1</sup>H spectrum showed the presence of broad signals at 37, 28, and 23 ppm and a sharper one at 13 ppm (Figure S3), all of them typical of H<sub>β</sub> and H<sub>α</sub> protons, respectively, of Cys residues bound to a [2Fe-2S]<sup>2+</sup> cluster with an S = 0 electronic ground state.<sup>31,32</sup>

The band at 540 nm in the UV-vis spectrum of the mixture has higher intensity and is better resolved than those typically observed in plant ferredoxins and adrenodoxin/putidaredoxin proteins,<sup>33</sup> whose UV-vis spectra resemble that of [2Fe-2S]<sup>2+</sup> ISCA2. An intense band at around 540 nm is present in the [2Fe-2S]<sup>2+</sup> centers of the so-called “red paramagnetic” ferredoxins, that is, from *Clostridium pasteurianum* and *Azotobacter vinelandii*, also having all-cysteinylic ligands as found in plant ferredoxins and adrenodoxin/putidaredoxins.<sup>34,35</sup> The observed spectral changes originate from the formation of the ISCA2-IBA57 complex, where the [2Fe-2S] cluster is exclusively bound to the complex. Indeed, when the [2Fe-2S] ISCA2-IBA57 1:1 protein mixture was passed through an analytical gel filtration column and the fractions of peaks 1 and 3 collected, the UV-vis spectrum of peak 1 fractions showed the same visible bands as those observed before gel filtrating the [2Fe-2S]/apo ISCA2-IBA57 mixture, while the visible bands in peak 3 fractions were absent (Figure 2b). These results strongly support that, upon mixing [2Fe-2S]/apo ISCA2 with IBA57, [2Fe-2S] ISCA2 quantitatively forms a complex with IBA57 via a shared binding of a [2Fe-2S] cluster. In agreement with this model, the CD spectrum of the [2Fe-2S]<sup>2+</sup> cluster in the [2Fe-2S]/apo ISCA2-IBA57 mixture is significantly different from that of the [2Fe-2S]<sup>2+</sup> cluster in [2Fe-2S] ISCA2 (Figure 2c), indicating differences in the cluster coordination and/or in the chirality of the cluster environment of the [2Fe-2S]<sup>2+</sup> clusters in ISCA2-IBA57 heterodimer with respect to ISCA2 homodimer.

The cluster stability of [2Fe-2S] ISCA2-IBA57 vs [2Fe-2S] ISCA2 upon oxygen exposure was then investigated by UV-vis spectroscopy, exposing the holo protein samples to air and collecting UV-vis spectra every 30 min for 15 h. It resulted that the Fe-S cluster in [2Fe-2S] ISCA2 is gradually degraded over a period of ~5 h, indicating that it is oxidatively labile. A rapid decrease of the adsorption bands between 300 and 700 nm characteristic of the [2Fe-2S]<sup>2+</sup> center was, indeed, observed (Figure 2d), resulting in the complete loss of the cluster, as assessed from the UV-vis spectrum acquired after gel-filtrating the final air-exposed protein. In contrast, in the heterodimer, the typical adsorption bands of the [2Fe-2S]<sup>2+</sup> cluster increased in intensity upon oxygen exposure and then remained stable in air for a few days (Figure 2e). This indicates that IBA57, by binding to [2Fe-2S] ISCA2, stabilizes the [2Fe-2S]<sup>2+</sup> cluster against oxidative degradation. The observed increase of the Fe-S cluster adsorption bands may be due to the presence of a fraction of the ISCA2-IBA57 complex having the cluster in a reduced [2Fe-2S]<sup>+</sup> state, which, then, slowly oxidizes to the [2Fe-2S]<sup>2+</sup> state upon oxygen exposure. The absorption bands of biological reduced [2Fe-2S]<sup>+</sup> clusters typically have lower intensities than those of oxidized [2Fe-2S]<sup>2+</sup> centers.<sup>34</sup> Therefore, upon cluster oxidation, the

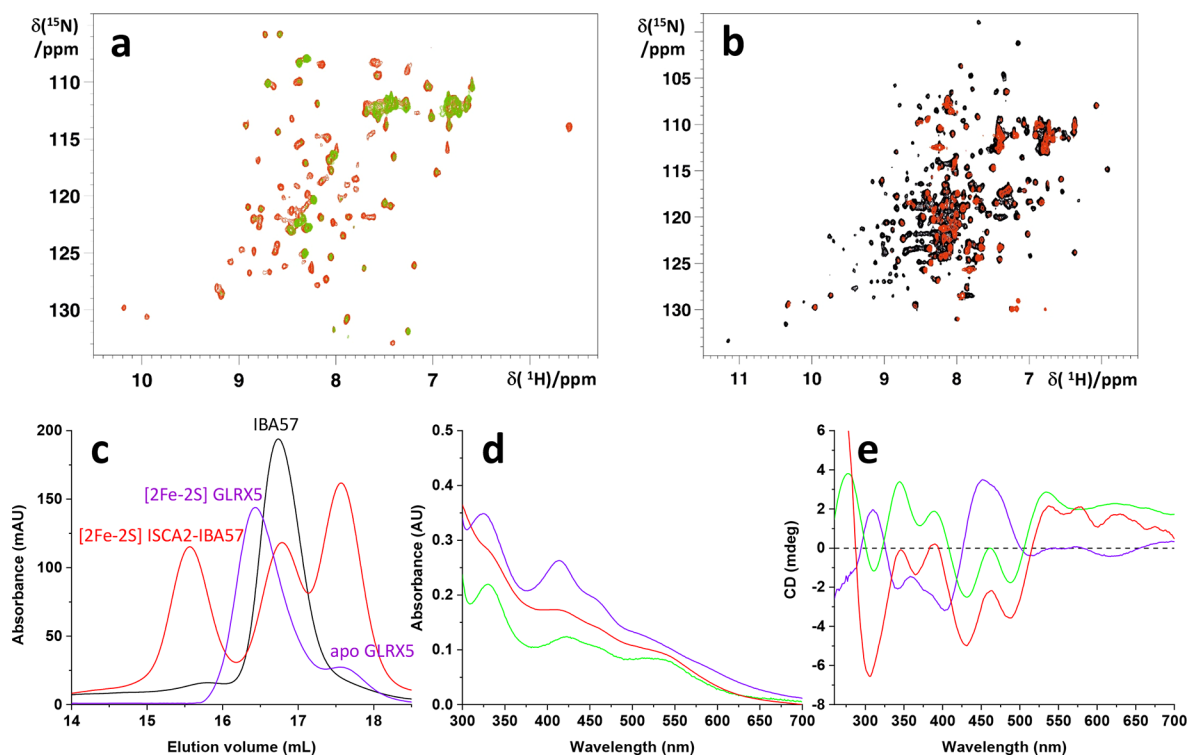


**Figure 3.** [2Fe-2S] ISCA2-IBA57 complex formation by mixing [2Fe-2S] GLRX5, apo ISCA2, and IBA57. Overlay of  $^1\text{H}$ - $^{15}\text{N}$  HSQC spectra: (a)  $^{15}\text{N}$ -labeled apo ISCA2 (0.6 mM) (red) and a 1:1:2 mixture of  $^{15}\text{N}$ -labeled apo ISCA2 (0.6 mM), unlabeled IBA57, unlabeled [2Fe-2S] $^{2+}$  GLRX5 (green), (b)  $^{15}\text{N}$ -labeled IBA57 (0.5 mM) (black) and a 1:1:2 mixture of  $^{15}\text{N}$ -labeled IBA57 (0.5 mM), unlabeled apo ISCA2, unlabeled [2Fe-2S] $^{2+}$  GLRX5 (red). (c) Elution profiles obtained for IBA57 (black), [2Fe-2S] $^{2+}$  GLRX5 (violet), a 1:1:1 mixture of apo ISCA2, IBA57 and [2Fe-2S] $^{2+}$  GLRX5 (red) by gel filtration on analytical Superdex<sup>TM</sup> 200 Increase 10/300 GL column. mAU: milli absorbance unit. UV-vis (d) and CD (e) spectra of [2Fe-2S] $^{2+}$  GLRX5 (violet), of the 1:1 [2Fe-2S]/apo ISCA2-IBA57 mixture (green), and of the 1:1:2 apo ISCA2-IBA57-[2Fe-2S] GLRX5 mixture (red). The experiments were conducted with monomeric protein concentration ranging from 0.15 mM to 0.6 mM depending on the applied spectroscopic technique.

intensities of the absorption bands of [2Fe-2S] $^{2+}$  cluster species are expected to increase, as experimentally observed in the UV-vis spectra acquired over time. In order to corroborate this hypothesis, we performed EPR measurements on [2Fe-2S] ISCA2-IBA57 before and after air exposure. The holo complex not exposed to air revealed an axial  $S = 1/2$  resonance with  $g_z < g_x = g_y$  ( $g_z = 2.01$ ,  $g_{\parallel} = 1.96$ ,  $g_{\text{av}} \sim 1.99$  at 45 K, Figure 2g), with relaxation properties characteristic of a reduced [2Fe-2S] $^{+}$  cluster. The  $g_{\text{av}}$  value is comparable to those of [2Fe-2S] $^{+}$  centers with complete cysteinyl ligation (typically  $g_{\text{av}} \sim 1.97$ ).<sup>36,37</sup> These EPR signals completely disappeared once the sample is exposed to air overnight (Figure 2h), and, upon dithionite reduction, the same signal reappeared (Figure 2i), indicating that the [2Fe-2S] center in the complex can undergo reversible redox cycling. Overall, the data demonstrate that the ISCA2-IBA57 complex can stabilize both reduced [2Fe-2S] $^{+}$  and oxidized [2Fe-2S] $^{2+}$  bound clusters.

The complex formation between [2Fe-2S] ISCA2 and IBA57 was also investigated by analyzing a protein mixture containing apo ISCA2, IBA57, and the physiological [2Fe-2S] cluster donor of ISCA proteins, that is, human GLRX5, which bridges an oxidized [2Fe-2S] $^{2+}$  cluster in a symmetric dimer, coordinating it by two glutathione molecules and two Cys ligands, one from each GLRX5 subunit.<sup>23,38</sup>  $^1\text{H}$ - $^{15}\text{N}$  HSQC NMR experiments were performed on a 1:1 apo ISCA2-IBA57 mixture,  $^{15}\text{N}$ -labeled in ISCA2 or in IBA57, titrated with unlabeled human [2Fe-2S] $^{2+}$  GLRX5. Stepwise additions of [2Fe-2S] $^{2+}$  GLRX5 to the apo ISCA2-IBA57 1:1 mixture cause

the NH cross-peaks broadening, until most of them disappear once 2 equiv of [2Fe-2S] $^{2+}$  GLRX5 were added (Figure 3a,b). Analytical gel filtration performed on the 1:1:1 apo ISCA2-IBA57-[2Fe-2S] GLRX5 mixture of the NMR titration showed the formation of the same peak as that observed by mixing [2Fe-2S]/apo ISCA2 with IBA57, which corresponds to the [2Fe-2S] ISCA2-IBA57 complex (Figure 3c). These data support the claim that the broadening effects observed for the backbone NHs in the  $^1\text{H}$ - $^{15}\text{N}$  HSQC experiments are determined by the formation of the large molecular mass protein complex of ISCA2 and IBA57. Analytical gel filtration data also showed the formation of apo GLRX5, whose peak increases in intensity in the 1:1:1 mixture, to the expense of dimeric [2Fe-2S] GLRX5, whose peak is not present in the 1:1:1 mixture (Figure 3c). UV-vis and CD spectra of the final mixture indicated the formation of the [2Fe-2S] ISCA2-IBA57 complex. They showed, indeed, the same bands as those described above (Figure 3d,e). The only difference with respect to the [2Fe-2S]/apo ISCA2-IBA57 mixture is observed in the EPR measurements. Indeed, no EPR signal was observed at 45 K in the final ISCA2-IBA57-GLRX5 mixture, indicating that only an oxidized [2Fe-2S] $^{2+}$  cluster is bound to the ISCA2-IBA57 complex. Overall, we can conclude that the oxidized [2Fe-2S] $^{2+}$  cluster is transferred from GLRX5 to ISCA2, which then forms the [2Fe-2S] $^{2+}$ -bound complex with IBA57.

**ISCA1 Does Not Form a Cluster-Mediated Complex with IBA57.** The possible cluster-mediated interaction of

IBA57 with ISCA1 was investigated by analytical gel filtration, UV–vis absorption, and CD spectroscopies. When IBA57 is mixed with apo ISCA1, analytical gel filtration of the protein mixture at 1:1 protein ratio did not show the presence of any peak at elution volumes higher than those of monomeric IBA57 and apo ISCA1 (Figure S4). Therefore, no complex formation occurs between the two proteins, as found in the case of apo ISCA2-IBA57 interaction. The 1:1 apo ISCA1-IBA57 mixture was then chemically reconstituted, and UV–vis and CD spectra recorded and compared with those of chemically reconstituted [2Fe-2S] ISCA2-IBA57 complex and [2Fe-2S] ISCA1. These data indicated that no cluster-mediated ISCA1-IBA57 heterocomplex is formed. Indeed, both UV–vis and CD spectra resemble those of [2Fe-2S] ISCA1. Specifically, the band at 540 nm, which is a marker of the formation of the [2Fe-2S] ISCA2-IBA57 heterocomplex, is not present in the UV–vis spectrum of the chemically reconstituted 1:1 ISCA1-IBA57 mixture (Figure S4). Consistent with no complex formation, the analytical gel filtration of the latter mixture did not show the presence of any peak at elution volumes higher than those of monomeric IBA57 and apo ISCA1 (Figure S4). Furthermore, a rapid decrease of the adsorption bands between 300 and 700 nm characteristic of the [2Fe-2S]<sup>2+</sup> center was observed upon oxygen exposure, as found in [2Fe-2S] ISCA2 and in contrast to what happened in the case of the [2Fe-2S] ISCA2-IBA57 complex.

Overall, these data indicate that ISCA2, and not ISCA1, specifically interacts with IBA57 to form a cluster-mediated interaction. They support the model proposed by Beilschmidt et al.,<sup>19</sup> which indicated that ISCA2, and not ISCA1, is complexed *in vivo* with IBA57. However, we cannot *a priori* exclude that, in some type of human cells or specific cellular conditions, even ISCA1 and IBA57 might cooperate in Fe-S protein maturation processes.

**Structure of IBA57 and Cluster Coordination in ISCA2-IBA57.** The crystal structure of IBA57 was determined at 1.75 Å resolution. IBA57 has a globular shape and consists of three tightly packed domains arranged in a rigid ring-like structure (Figure 4a). Only the regions on the protein surface have very poor electron density or high B-factors (Figure S5). Domain A includes residues 17–25 and 127–185 and is formed by a five-stranded antiparallel  $\beta$ -sheet and a short  $\alpha$ -helix on one side of the sheet (yellow domain in Figure 4a). Domain B includes residues 26–126 and may be considered as an insertion in domain A. It is formed by a five-stranded antiparallel  $\beta$ -sheet and two  $\alpha$ -helices on one side of the  $\beta$ -sheet (gray domain in Figure 4a). Domain C comprises 77 C-terminal residues; it has the topology of a six-strand antiparallel  $\beta$ -barrel with a Greek key connection pattern, and packs perpendicular to the  $\beta$ -sheets of domains A and B, closing the protein ring-like structure (red domain in Figure 4a). A 60-residue segment (residues 186 to 246) is sandwiched among the three domains and, with the exception of two long  $\alpha$ -helices and one short  $3_{10}$ -helix, lacks secondary structure elements (dark green domain in Figure 4a).

The 60-residue segment comprises the sequence motif KGC(Y/F)XGQE conserved in the COG0354 protein family, which is located in the region connecting the short  $3_{10}$ -helix with the subsequent long  $\alpha$ -helix of this segment (Figure 4a). The conserved sequence motif is well-packed to domain B via hydrophobic interactions (Figure 4b). As a result, the fully conserved Cys 230 of the KGC(Y/F)XGQE sequence motif resides highly exposed to the solvent and in a well-structured

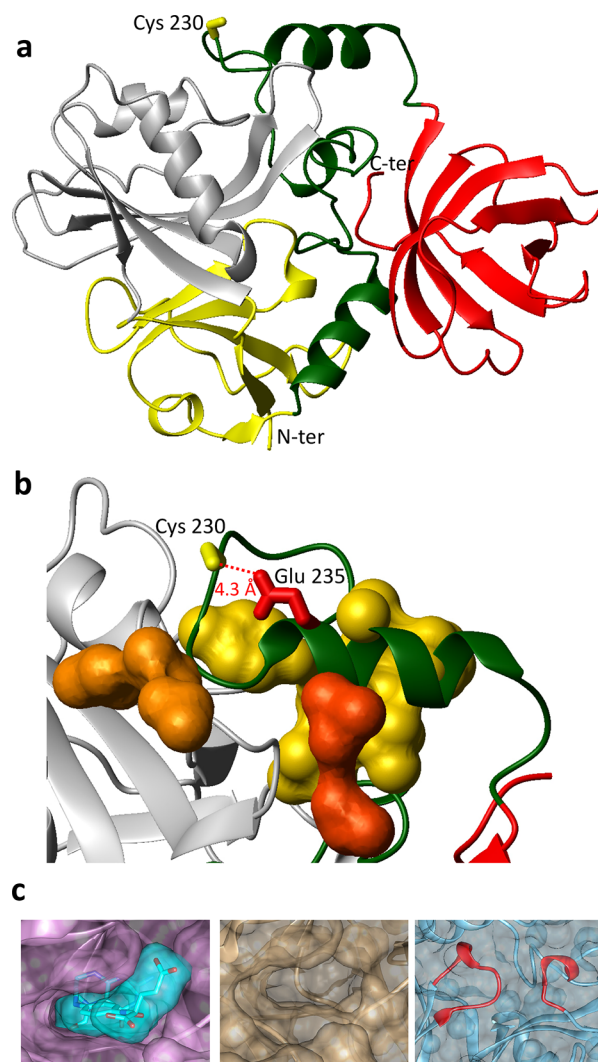


**Figure 4.** Crystal structure of IBA57. (a) Ribbon diagram of IBA57 with domains A, B, and C colored in yellow, gray, and red, respectively. The 60-residue segment sandwiched among the three domains is in dark green. (b) The region containing the conserved sequence motif KGC(Y/F)XGQE, is well-packed to domain B via hydrophobic interactions defined by three patches: Val 73, Ile 232, and Leu 44 (vdW side-chains in orange); Leu 214, Leu 218, Ala 219, Tyr 231, Val 224, Phe 226, His 241, and Ala 238 (vdW side-chains in yellow); Leu 212 and Leu 236 (vdW side-chains in red). (c) Transparent molecular surfaces of the tetrahydrofolate binding site/cavity in aminomethyl-transferase (on the left, the folinic acid-bound structure (PDB ID 1WOP) and, in the center, the apo structure (PDB ID 1WOS)), and, on the right, of the corresponding region in IBA57 structure. A loop of domain A and the  $3_{10}$ -helix of the 60-residue segment of IBA57 are shown in red.

and rigid region (Figure 4b). The IBA57 structure supports a possible role of Cys 230 as a ligand of the [2Fe-2S] cluster, bridging the two proteins.

In order to corroborate such hypothesis, Cys 230 was substituted with Ala, the crystal structure of Cys230Ala IBA57 was determined, and the holo complex formation was investigated by SEC-MALS, and UV–vis, and CD spectroscopies. The structure of Cys230Ala IBA57 showed that the Cys to Ala substitution does not perturb neither protein fold nor the backbone and side chain conformations of the residues of the KGC(Y/F)XGQE motif containing Cys 230 (Figure

SS). A 1:1 mixture of Cys230Ala IBA57 mutant and apo ISCA2 was chemically reconstituted with the same conditions as those used for the wild-type protein. SEC-MALS of this mixture showed that no complex is formed, while the peak of IBA57 was still largely present in the mixture, at variance with what was observed for the wild-type complex (Figure 5a). A very broad and weak peak (peak 4) with a molar mass of 43.1

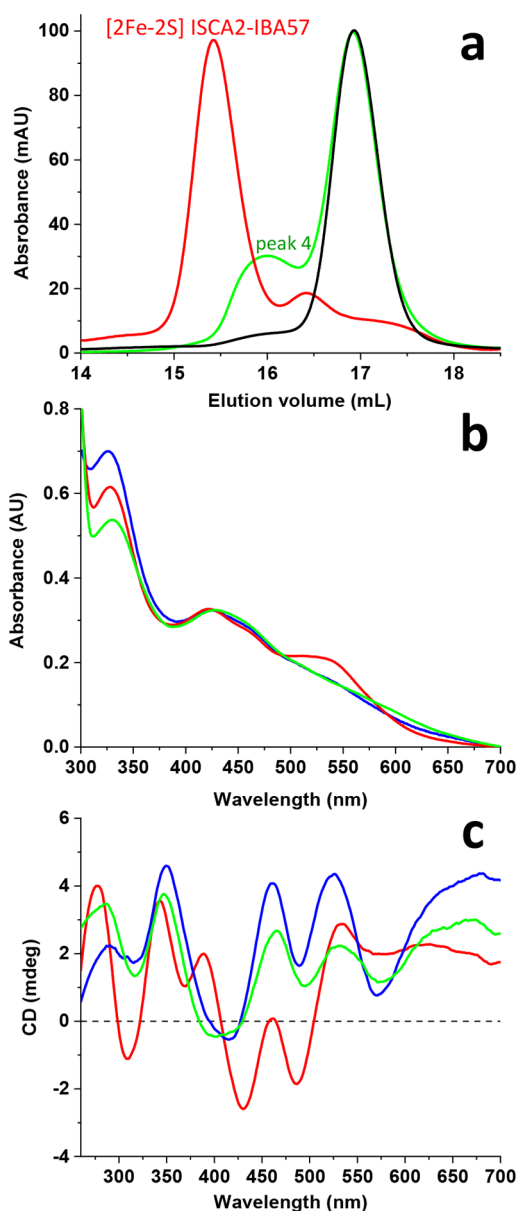


**Figure 5.** Cys 230 to Ala substitution affects the [2Fe-2S] ISCA2-IBA57 complex formation. (a) Elution profiles obtained for IBA57 (black), the 1:0.5 [2Fe-2S]/apo ISCA2-IBA57 mixture (red), and the 1:1 mixture of Cys230Ala IBA57 mutant and apo ISCA2 chemically reconstituted with the same conditions as those used for the wild-type complex (green) by gel filtration on analytical Superdex<sup>TM</sup> 200 Increase 10/300 GL column. mAU: milli absorbance unit. UV-vis (b) and CD (c) spectra of chemically reconstituted ISCA2-Cys230Ala IBA57 1:1 mixture (green), of chemically reconstituted [2Fe-2S] ISCA2 (blue), and of chemically reconstituted [2Fe-2S] ISCA2-IBA57 (red). The experiments were conducted with monomeric protein concentration of ISCA2 ranging from 0.15 mM to 0.6 mM depending on the applied spectroscopic technique.

$\pm 3.5$  kDa elutes in between the peaks of [2Fe-2S] ISCA2 and [2Fe-2S] ISCA2-IBA57 (Figure 5a and Figure S1), suggesting that the Cys-to-Ala substitution affects the complex formation in terms of geometrical dimensions and yield, the latter being drastically reduced. The UV-vis spectrum of the chemically reconstituted ISCA2-Cys230Ala IBA57 mixture has the typical bands of [2Fe-2S] ISCA2 and lacks the band at 540 nm typical of the [2Fe-2S] ISCA2-IBA57 complex (Figure 5b). In addition, the CD spectrum of the chemically reconstituted ISCA2-Cys230Ala IBA57 mixture essentially showed the same bands as those observed in [2Fe-2S] ISCA2 and not those of the [2Fe-2S] ISCA2-IBA57 complex (Figure 5c). Finally, the cluster stability upon air exposure of the chemically reconstituted ISCA2-Cys230Ala IBA57 is the same as that observed for [2Fe-2S] ISCA2, that is, the Fe-S cluster is oxidatively labile and gradually degraded over a period of  $\sim 5$  h (Figure 2f). In conclusion, the substitution of Cys 230 largely abolished the formation of the [2Fe-2S] heterocomplex and consequently the oxygen resistance of the cluster. These data strongly support the participation of Cys 230 in cluster coordination. To further confirm this, we have performed a AMS-based alkylation gel shift assay, which showed that one of the four cysteines of IBA57 (i.e., Cys 230) is not available to be alkylated in the [2Fe-2S] ISCA2-IBA57 complex with respect to the uncomplexed IBA57 (Figure S6). This result suggested that Cys 230 cannot be alkylated by AMS once it is involved in cluster binding. From both site-directed mutagenesis and AMS results, we conclude that Cys 230 of IBA57 is involved in the cluster binding in the [2Fe-2S] complex.

Since no further potential [2Fe-2S] cluster ligands (i.e., Cys and His) from IBA57 are within 6 Å to Cys 230, we expect that the other three cluster ligands in [2Fe-2S] ISCA2-IBA57 result from ISCA2, and they might be the three cysteine cluster ligands conserved in the ISCA protein family (i.e., Cys 79, Cys 144 and Cys 146 in ISCA2).<sup>20,22,39</sup> To investigate whether they are involved in cluster binding in the ISCA2-IBA57 complex, we produced three ISCA2 mutants in which either Cys 79 or Cys 144 or Cys 146 were substituted with Ser. Three 1:1 mixtures of IBA57 with each single apo ISCA2 mutant were then chemically reconstituted following the same procedure used for the wild-type protein, and UV-vis and analytical gel filtration data were collected and compared with those of [2Fe-2S] ISCA2-IBA57. Analytical gel filtration of any of the three mixtures showed that the [2Fe-2S] ISCA2-IBA57 complex is not formed in any case, while the peak of isolated IBA57 is still largely present in each mixture (Figure 6a). Specifically, in Cys144Ser ISCA2, a very broad and weak peak (peaks 4' in Figure 6a), the same as that observed in the chemically reconstituted 1:1 mixture of Cys230Ala IBA57 and apo ISCA2 (peak 4 in Figure 5a), is present in which the Fe-S cluster is oxidatively labile and gradually degraded over a period of  $\sim 5$  h. In the mixtures with Cys79Ser and Cys146Ser ISCA2, no peak at elution volumes higher than those of IBA57 and apo ISCA2 is present (Figure 6a), similarly to what it was observed in the apo ISCA2-IBA57 mixture (Figure 1a). On the basis of these results we can propose that all the three cysteines are required for the binding of the [2Fe-2S] cluster which bridges the two proteins. The UV-vis spectra of the three chemically reconstituted mixtures of any ISCA2 mutant with IBA57s corroborate such a model. Indeed, they do not show the band at 540 nm, which is the characteristic fingerprint for the formation of the [2Fe-2S] ISCA2-IBA57 complex (Figure 6b). This indicates that the [2Fe-2S] ISCA2-IBA57 complex is

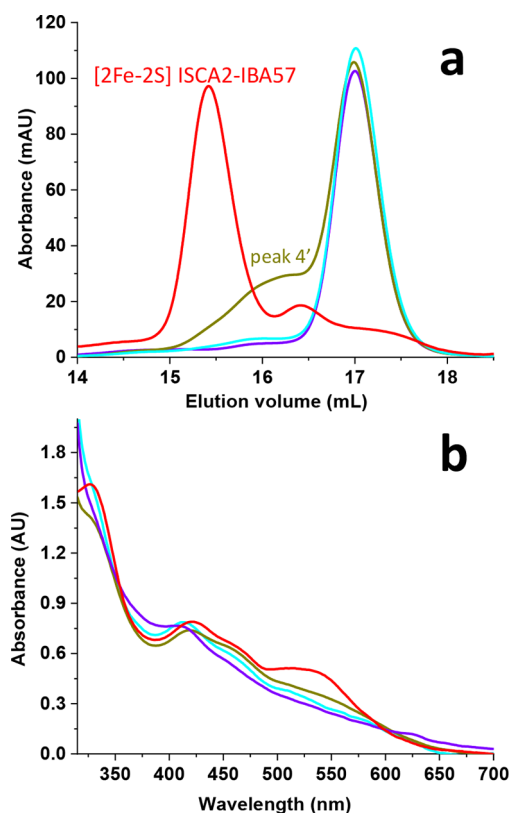


**Figure 6.** Cys 79, Cys 144, and Cys 146 to Ser substitutions affect the [2Fe-2S] ISCA2-IBA57 complex formation. (a) Elution profiles obtained for chemically reconstituted Cys79Ser ISCA2-IBA57 1:1 mixture (violet), Cys144Ser ISCA2-IBA57 1:1 mixture (dark yellow), Cys146Ser ISCA2-IBA57 1:1 mixture (cyano), and the 1:0.5 [2Fe-2S]/apo ISCA2-IBA57 mixture (red) by gel filtration on analytical SuperdexTM 200 Increase 10/300 GL column. mAU: milli absorbance unit. (b) UV-vis spectra of chemically reconstituted 1:1 mixtures of Cys79Ser with IBA57 (violet), Cys144Ser ISCA2 with IBA57 (dark yellow), Cys146Ser ISCA2 with IBA57 (cyano), and [2Fe-2S]/apo ISCA2 with IBA57 (red). Monomeric protein concentration of ISCA2 mutants was 0.2 mM.

not formed upon mutation of any of the ISCA2 cysteine, pointing at the importance of all three cysteines for ligating the cluster in the heterocomplex. The UV-vis spectrum of each of the three mixtures (Figure 6b) showed the presence of a cluster-bound species, which is due to the formation, upon chemical reconstitution, of the holo species of each ISCA2 mutant. Indeed, these UV-vis spectra of the mixture with any of the three mutants match those of the three chemically reconstituted ISCA2 mutants alone, previously reported.<sup>22</sup>

In conclusion, the [2Fe-2S] ISCA2-IBA57 complex formation is abolished in any of the three mutants, similarly to what it occurs once Cys 230 of IBA57 is substituted by Ala. From these data we can propose that the [2Fe-2S] cluster in the ISCA2-IBA57 complex is asymmetrically coordinated by Cys 79, Cys 144, and Cys 146 from ISCA2 and Cys 230 from IBA57. Such coordination in the heterodimeric ISCA2-IBA57 complex could be achieved, along the interaction between IBA57 and dimeric [2Fe-2S] ISCA2, through the displacement of Cys 79 and Cys 146 from one subunit of [2Fe-2S] ISCA2, which is thus released in solution, by Cys 230 of IBA57 and by Cys 146 of the other ISCA2 subunit.

**IBA57 Does Not Bind Tetrahydrofolate Derivatives.** It has been proposed that tetrahydrofolates play a role in the

metabolism of iron-sulfur clusters in all domains of life by participating in the assembly or repair of Fe-S clusters and that IBA57 protein family acts as the direct link between tetrahydrofolates and Fe-S cluster enzymes by showing a folate binding site.<sup>16,40,41</sup> This proposal stems from experimental data on *E. coli* IBA57 homologue, that is, YgfZ protein.<sup>16,42</sup> IBA57 structure is similar to that of YgfZ<sup>43</sup> as well as to an aminomethyl-transferase involved in the mitochondrial glycine cleavage system<sup>44</sup> and to the C-terminal domain of a mammalian dimethylglycine dehydrogenase.<sup>45</sup> The two latter proteins bind tetrahydrofolate in a large central cavity, with the pterin ring of tetrahydrofolate located in the center of the cavity and the glutamate tail exposed to the external solvent (Figure 4c). This cavity is preserved in the apo proteins, indicating the presence of a rigid tetrahydrofolate binding pocket (Figure 4c). The YgfZ protein has been also shown to bind tetrahydrofolate, potentially in the same cavity, but with lower affinity than that typically observed for binding of folate substrates.<sup>16,43</sup> This central cavity is absent in IBA57, as a consequence of a backbone conformation of a loop of domain A and of the  $3_{10}$ -helix of the 60-residue segment different from the same regions in the structural homologues (Figure 4c). Moreover, the residues typically involved in the interaction between tetrahydrofolate and the aminomethyl-transferase/dimethylglycine dehydrogenase proteins<sup>44,45</sup> are not conserved in IBA57. <sup>1</sup>H 1D ePHOGSY NMR experiments and <sup>1</sup>H-<sup>15</sup>N HSQC NMR titrations between IBA57 and tetrahydrofolate derivatives as well as <sup>1</sup>H 1D ePHOGSY NMR experiments between the [2Fe-2S] ISCA2-IBA57 complex and calcium folinate showed no significant peak intensity variation in the 1D NMR experiments and no chemical shift changes in <sup>1</sup>H-<sup>15</sup>N HSQC maps of <sup>15</sup>N-labeled IBA57 (Figure S7), indicating no interaction between free and complexed IBA57 and the tetrahydrofolate derivatives. From both the structural and interaction data, we conclude that tetrahydrofolate derivatives are not substrates of IBA57.

**[2Fe-2S] ISCA2-IBA57 Reactivates Apo Aconitase.** The oxygen resistance of the cluster in [2Fe-2S] ISCA2-IBA57 suggests that the heterocomplex might operate under aerobic cellular conditions, possibly being involved in the reactivation of mitochondrial Fe-S enzymes. It was well established, indeed, that Fe-S clusters of mitochondrial enzymes, such as that of aconitase, can fully disassemble upon exposure to oxidants.<sup>46,47</sup> Therefore, we have tested *in vitro* whether [2Fe-2S] ISCA2-IBA57 can recycle apo aconitase into [4Fe-4S] aconitase. To do that, aerobically purified cytosolic aconitase, which contains residual amounts of [4Fe-4S] bound cluster according to UV-vis and activity measurement (Figure S8), was anaerobically incubated with the [2Fe-2S] ISCA2-IBA57 complex for 45 min at 25 °C, and then aconitase activity was measured following a previously reported protocol.<sup>25</sup> The mixture showed increased activity with respect to that of untreated aconitase and is ~70% of that obtained by the chemically reconstituted aconitase (Figure S8). We also verified that [2Fe-2S] ISCA2-IBA57 alone does not experience citrate/isocitrate activity. These data indicate that the [2Fe-2S] ISCA2-IBA57 is able to reactivate apo aconitase.

## DISCUSSION

Human IBA57 is required for the maturation of mitochondrial [4Fe-4S] proteins (i.e., aconitase, respiratory complex I, succinate dehydrogenase, and lipoic acid synthase) in HeLa cells, while the function of the mitochondrial [2Fe-2S]

ferrochelatase was unaffected by IBA57.<sup>11</sup> On this basis, it was proposed that IBA57 is specifically required for the generation of [4Fe-4S] clusters and their dedicated insertion into mitochondrial apo recipient proteins. This function has been found to be strictly related to two other proteins of the mitochondrial ISC assembly machinery, that is, ISCA1 and ISCA2, which showed the same phenotype as that of IBA57 in HeLa cells.<sup>11</sup> From those studies, it was concluded that the three proteins work together in a complex to assemble a [4Fe-4S] cluster.<sup>18</sup> This model was indirectly corroborated by the fact that very similar phenotypes for the three proteins were also found in yeast and by the finding that yeast Iba57 physically interacts with yeast Isa1 and Isa2.<sup>12,15</sup> This stringent functional association has been, however, revisited in a recent study, which showed that ISCA2 and IBA57 are not required under standard physiological conditions for the maturation of mitochondrial [4Fe-4S] proteins in mouse skeletal muscle and in primary cultures of neurons and that ISCA2, but not ISCA1, interacts with IBA57.<sup>19</sup>

Our work shows that IBA57 forms a heterodimeric complex with ISCA2, and not with ISCA1, by bridging a [2Fe-2S] cluster that is resistant to highly oxidative environments. Specifically, this complex is the final product when IBA57 is either exposed to [2Fe-2S] ISCA2 or in the presence of [2Fe-2S] GLRX5 and apo ISCA2. The latter results suggest that a cluster transfer pathway involving three partner proteins of the mitochondrial ISC machinery (GLRX5, ISCA2, and IBA57) is operative. This pathway starts with [2Fe-2S] cluster transfer from [2Fe-2S] GLRX5 to ISCA2 and ends up with the formation of a [2Fe-2S] cluster-mediated ISCA2-IBA57 complex. Cluster binding is, indeed, absolutely required to promote complex formation between ISCA2 and IBA57 proteins. No formation of a [4Fe-4S] cluster bound to the ISCA2-IBA57 complex was observed along this pathway, at variance with what it was observed in the interaction of [2Fe-2S] GLRX5 with the apo ISCA1-ISCA2 complex that is able to form a [4Fe-4S] cluster.<sup>20,22</sup> We also identified Cys 230 of IBA57 and Cys 79, Cys 144, and Cys 146 of ISCA2 as the ligands bridging the [2Fe-2S] cluster between the two proteins and showed that all cysteines are required to stabilize the complex formation and the [2Fe-2S] cluster against oxidative degradation.

The stability of the [2Fe-2S] cluster against oxidative degradation, observed upon its binding to the ISCA2-IBA57 complex with respect to when it is bound to ISCA2 alone, supports a model where the heterocomplex can work under aerobic cellular conditions. This model fits well with the experimental and genomic data that connect COG0354 proteins with aerobic organisms and oxidative stress.<sup>16,48</sup> Moreover, this model agrees with what has been recently suggested on the basis of a cell-dependent phenotype observed for both ISCA2 and IBA57,<sup>11,19</sup> namely that ISCA2 and IBA57 might be activated together for Fe-S biogenesis upon specific cellular conditions, such as cell proliferation (a process requiring adequate oxygen concentrations to be effective) and oxidative stress.<sup>19</sup> We also found that the [2Fe-2S] ISCA2-IBA57 complex is able to substantially reactivate *in vitro* human aconitase. This indicates that the [2Fe-2S] heterocomplex is able to mature aconitase by providing a [4Fe-4S] cluster. It is possible that the ability of the heterocomplex to stabilize both reduced and oxidized states of the [2Fe-2S] cluster drives a reductive coupling of two reduced [2Fe-2S]<sup>+</sup> clusters into an oxidized [4Fe-4S]<sup>2+</sup> cluster<sup>49,50</sup> on aconitase. The binding

preference, in the ISCA2-IBA57 complex, of a [2Fe-2S] cluster over a [4Fe-4S] cluster might be explained by the fact that aerobic organisms have favored the use of the more chemically stable [2Fe-2S] clusters than the more damageable [4Fe-4S] clusters.<sup>51</sup> In conclusion, the [2Fe-2S] ISCA2-IBA57 complex may be required as a specific system maturing Fe-S enzymes under aerobic cellular conditions, similarly to what observed in the cytosol of human cells, where the [2Fe-2S] form of mitoNEET is resistant to oxidants and is capable of reactivating cytosolic aconitase.<sup>52–54</sup>

## ■ ASSOCIATED CONTENT

### § Supporting Information

The Supporting Information is available free of charge on the ACS Publications website at DOI: 10.1021/jacs.8b09061.

Figures S1–S8 (PDF)

## ■ AUTHOR INFORMATION

### Corresponding Authors

\*banci@cerm.unifi.it

\*ciofi@cerm.unifi.it

### ORCID

Vito Calderone: 0000-0002-7963-6241

Simone Ciofi-Baffoni: 0000-0002-2376-3321

Lucia Banci: 0000-0003-0562-5774

### Author Contributions

<sup>§</sup>These authors contributed equally

### Notes

The authors declare no competing financial interest.

## ■ ACKNOWLEDGMENTS

The authors acknowledge the support and the use of resources of Instruct-ERIC, a Landmark ESFRI project, and specifically the CERM/CIRMMP Italy Centre. This work has also been supported by iNEXT, grant number 653706, funded by the Horizon 2020 programme of the European Commission. This article is based upon work from COST Action CA15133, supported by the European Cooperation in Science and Technology (COST).

## ■ REFERENCES

- (1) Rouault, T. A. Mammalian iron-sulphur proteins: novel insights into biogenesis and function. *Nat. Rev. Mol. Cell Biol.* **2015**, *16* (1), 45–55.
- (2) Sheftel, A.; Stehling, O.; Lill, R. Iron-sulfur proteins in health and disease. *Trends Endocrinol. Metab.* **2010**, *21* (5), 302–314.
- (3) Beilschmidt, L. K.; Puccio, H. M. Mammalian Fe-S cluster biogenesis and its implication in disease. *Biochimie* **2014**, *100*, 48–60.
- (4) Ciofi-Baffoni, S.; Nasta, V.; Banci, L. Protein networks in the maturation of human iron-sulfur proteins. *Metallomics* **2018**, *10*, 49–72.
- (5) Stehling, O.; Wilbrecht, C.; Lill, R. Mitochondrial iron-sulfur protein biogenesis and human disease. *Biochimie* **2014**, *100*, 61–77.
- (6) Kaut, A.; Lange, H.; Diekert, K.; Kispal, G.; Lill, R. Isa1p is a component of the mitochondrial machinery for maturation of cellular iron-sulfur proteins and requires conserved cysteine residues for function. *J. Biol. Chem.* **2000**, *275* (21), 15955–15961.
- (7) Pelzer, W.; Muhlenhoff, U.; Diekert, K.; Siegmund, K.; Kispal, G.; Lill, R. Mitochondrial Isa2p plays a crucial role in the maturation of cellular iron-sulfur proteins. *FEBS Lett.* **2000**, *476* (3), 134–139.
- (8) Cozar-Castellano, I.; del Valle, M. M.; Trujillo, E.; Arteaga, M. F.; Gonzalez, T.; Martin-Vasallo, P.; Avila, J. hIsca: a protein

implicated in the biogenesis of iron-sulfur clusters. *Biochim. Biophys. Acta, Proteins Proteomics* **2004**, *1700*, 179–188.

(9) Rodriguez-Manzanique, M. T.; Tamarit, J.; Belli, G.; Ros, J.; Herrero, E. Grx5 is a mitochondrial glutaredoxin required for the activity of iron/sulfur enzymes. *Mol. Biol. Cell* **2002**, *13* (4), 1109–1121.

(10) Vilella, F.; Alves, R.; Rodriguez-Manzanique, M. T.; Belli, G.; Swaminathan, S.; Sunnerhagen, P.; Herrero, E. Evolution and cellular function of monothiol glutaredoxins: involvement in iron-sulphur cluster assembly. *Comp. Funct. Genomics* **2004**, *5* (4), 328–341.

(11) Sheftel, A. D.; Wilbrecht, C.; Stehling, O.; Niggemeyer, B.; Elsasser, H. P.; Muhlenhoff, U.; Lill, R. The human mitochondrial ISCA1, ISCA2, and IBA57 proteins are required for [4Fe-4S] protein maturation. *Mol. Biol. Cell* **2012**, *23* (7), 1157–1166.

(12) Muhlenhoff, U.; Richter, N.; Pines, O.; Pierik, A. J.; Lill, R. Specialized function of yeast Isa1 and Isa2 proteins in the maturation of mitochondrial [4Fe-4S] proteins. *J. Biol. Chem.* **2011**, *286* (48), 41205–41216.

(13) Muhlenhoff, U.; Gerl, M. J.; Flauger, B.; Pirner, H. M.; Balsler, S.; Richhardt, N.; Lill, R.; Stolz, J. The ISC proteins Isa1 and Isa2 are required for the function but not for the de novo synthesis of the Fe/S clusters of biotin synthase in *Saccharomyces cerevisiae*. *Eukaryotic Cell* **2007**, *6*, 495–504.

(14) Kim, K. D.; Chung, W. H.; Kim, H. J.; Lee, K. C.; Roe, J. H. Monothiol glutaredoxin Grx5 interacts with Fe-S scaffold proteins Isa1 and Isa2 and supports Fe-S assembly and DNA integrity in mitochondria of fission yeast. *Biochem. Biophys. Res. Commun.* **2010**, *392* (3), 467–472.

(15) Gelling, C.; Dawes, I. W.; Richhardt, N.; Lill, R.; Muhlenhoff, U. Mitochondrial Iba57p is required for Fe/S cluster formation on aconitase and activation of radical SAM enzymes. *Mol. Cell. Biol.* **2008**, *28* (5), 1851–1861.

(16) Waller, J. C.; Alvarez, S.; Naponelli, V.; Lara-Nunez, A.; Blaby, I. K.; Da Silva, V.; Ziemak, M. J.; Vickers, T. J.; Beverley, S. M.; Edison, A. S.; Rocca, J. R.; Gregory, J. F., III; Crecy-Lagard, V.; Hanson, A. D. A role for tetrahydrofolates in the metabolism of iron-sulfur clusters in all domains of life. *Proc. Natl. Acad. Sci. U. S. A.* **2010**, *107* (23), 10412–10417.

(17) Andreini, C.; Banci, L.; Rosato, A. Exploiting bacterial operons to illuminate human iron-sulfur proteins. *J. Proteome Res.* **2016**, *15*, 1308–1322.

(18) Braymer, J. J.; Lill, R. Iron-sulfur cluster biogenesis and trafficking in mitochondria. *J. Biol. Chem.* **2017**, *292* (31), 12754–12763.

(19) Beilschmidt, L. K.; Ollagnier de Choudens, S.; Fournier, M.; Sanakis, I.; Hograindleur, M. A.; Clemancey, M.; Blondin, G.; Schmucker, S.; Eisenmann, A.; Weiss, A.; Koebel, P.; Messaddeq, N.; Puccio, H.; Martelli, A. ISCA1 is essential for mitochondrial Fe4S4 biogenesis in vivo. *Nat. Commun.* **2017**, *8*, 15124.

(20) Brancaccio, D.; Gallo, A.; Mikolajczyk, M.; Zovo, K.; Palumaa, P.; Novellino, E.; Piccioli, M.; Ciofi-Baffoni, S.; Banci, L. Formation of [4Fe-4S] clusters in the mitochondrial iron-sulfur cluster assembly machinery. *J. Am. Chem. Soc.* **2014**, *136* (46), 16240–16250.

(21) Torracco, A.; Ardisson, A.; Invernizzi, F.; Rizza, T.; Fiermonte, G.; Niceta, M.; Zanetti, N.; Martinelli, D.; Voza, A.; Verrigni, D.; Di Nottia, M.; Lamantea, E.; Diodato, D.; Tartaglia, M.; Dionisi-Vici, C.; Moroni, I.; Farina, L.; Bertini, E.; Ghezzi, D.; Carrozzo, R. Novel mutations in IBA57 are associated with leukodystrophy and variable clinical phenotypes. *J. Neurol.* **2017**, *264* (1), 102–111.

(22) Brancaccio, D.; Gallo, A.; Piccioli, M.; Novellino, E.; Ciofi-Baffoni, S.; Banci, L. [4Fe-4S] Cluster Assembly in Mitochondria and Its Impairment by Copper. *J. Am. Chem. Soc.* **2017**, *139*, 719–730.

(23) Banci, L.; Brancaccio, D.; Ciofi-Baffoni, S.; Del Conte, R.; Gadepalli, R.; Mikolajczyk, M.; Neri, S.; Piccioli, M.; Winkelmann, J. [2Fe-2S] cluster transfer in iron-sulfur protein biogenesis. *Proc. Natl. Acad. Sci. U. S. A.* **2014**, *111* (17), 6203–6208.

(24) Chen, J.; Acton, T. B.; Basu, S. K.; Montelione, G. T.; Inouye, M. Enhancement of the solubility of proteins overexpressed in

*Escherichia coli* by heat shock. *J. Mol. Microbiol. Biotechnol.* **2002**, *4* (6), 519–524.

(25) Maione, V.; Cantini, F.; Severi, M.; Banci, L. Investigating the role of the human CIA2A-CIAO1 complex in the maturation of aconitase. *Biochim. Biophys. Acta, Gen. Subj.* **2018**, *1862* (9), 1980–1987.

(26) Banci, L.; Bertini, I.; Cefaro, C.; Ciofi-Baffoni, S.; Gallo, A.; Martinelli, M.; Sideris, D. P.; Katrakili, N.; Tokatlidis, K. MIA40 is an oxidoreductase that catalyzes oxidative protein folding in mitochondria. *Nat. Struct. Mol. Biol.* **2009**, *16* (2), 198–206.

(27) Dalvit, C.; Hommel, U. New pulsed field gradient NMR experiments for the detection of bound water in proteins. *J. Biomol. NMR* **1995**, *5*, 306–310.

(28) Uzarska, M. A.; Dutkiewicz, R.; Freibert, S. A.; Lill, R.; Muhlenhoff, U. The mitochondrial Hsp70 chaperone Ssq1 facilitates Fe/S cluster transfer from Isu1 to Grx5 by complex formation. *Mol. Biol. Cell* **2013**, *24* (12), 1830–1841.

(29) Bandyopadhyay, S.; Gama, F.; Molina-Navarro, M. M.; Gualberto, J. M.; Claxton, R.; Naik, S. G.; Huynh, B. H.; Herrero, E.; Jacquot, J. P.; Johnson, M. K.; Rouhier, N. Chloroplast monothiol glutaredoxins as scaffold proteins for the assembly and delivery of [2Fe-2S] clusters. *EMBO J.* **2008**, *27* (7), 1122–1133.

(30) Noodleman, L.; Baerends, E. J. Electronic structure, magnetic properties, ESR and optical spectra for 2-Fe ferredoxin models by LCAO-Xa valence bond theory. *J. Am. Chem. Soc.* **1984**, *106*, 2316–2327.

(31) Banci, L.; Camponeschi, F.; Ciofi-Baffoni, S.; Piccioli, M. The NMR contribution to protein-protein networking in Fe-S protein maturation. *JBIC, J. Biol. Inorg. Chem.* **2018**, *23* (4), 665–685.

(32) Banci, L.; Bertini, I.; Luchinat, C. The <sup>1</sup>H NMR parameters of magnetically coupled dimers - The Fe<sub>2</sub>S<sub>2</sub> proteins as an example. *Struct. Bonding (Berlin)* **1990**, *72*, 113–135.

(33) Meyer, J.; Bruschi, M. H.; Bonicel, J. J.; Bovier-Lapierre, G. E. Amino acid sequence of [2Fe-2S] ferredoxin from *Clostridium pasteurianum*. *Biochemistry* **1986**, *25* (20), 6054–61.

(34) Han, S.; Czernuszewicz, R. S.; Kimura, T.; Adams, M. W. W.; Spiro, T. G. Fe<sub>2</sub>S<sub>2</sub> protein resonance Raman spectra revisited: structural variations among adrenodoxin, ferredoxin, and red paramagnetic protein. *J. Am. Chem. Soc.* **1989**, *111* (10), 3505–3511.

(35) Chatelet, C.; Meyer, J. The [2Fe-2S] protein I (Shetna protein I) from *Azotobacter vinelandii* is homologous to the [2Fe-2S] ferredoxin from *Clostridium pasteurianum*. *JBIC, J. Biol. Inorg. Chem.* **1999**, *4* (3), 311–7.

(36) Bertrand, P.; Guigliarelli, B.; More, C. The mixed-valence [Fe(III), Fe(II)] binuclear centers of biological molecules viewed through EPR spectroscopy. *New J. Chem.* **1991**, *15*, 445–454.

(37) Banci, L.; Ciofi-Baffoni, S.; Mikolajczyk, M.; Winkelmann, J.; Bill, E.; Pandelia, M. E. Human anamorsin binds [2Fe-2S] clusters with unique electronic properties. *JBIC, J. Biol. Inorg. Chem.* **2013**, *18*, 883–893.

(38) Johansson, C.; Roos, A. K.; Montano, S. J.; Sengupta, R.; Filippakopoulos, P.; Guo, K.; von Delft, F.; Holmgren, A.; Oppermann, U.; Kavanagh, K. L. The crystal structure of human GLRX5: iron-sulfur cluster co-ordination, tetrameric assembly and monomer activity. *Biochem. J.* **2011**, *433* (2), 303–311.

(39) Zheng, L.; Cash, V. L.; Flint, D. H.; Dean, D. R. Assembly of iron-sulfur clusters. Identification of an iscSUA-hscBA-fox gene cluster from *Azotobacter vinelandii*. *J. Biol. Chem.* **1998**, *273* (21), 13264–13272.

(40) Waller, J. C.; Ellens, K. W.; Alvarez, S.; Loizeau, K.; Ravel, S.; Hanson, A. D. Mitochondrial and plastidial COG0354 proteins have folate-dependent functions in iron-sulphur cluster metabolism. *J. Exp. Bot.* **2012**, *63* (1), 403–11.

(41) Waller, J. C.; Ellens, K. W.; Hasnain, G.; Alvarez, S.; Rocca, J. R.; Hanson, A. D. Evidence that the folate-dependent proteins YgfZ and MnmEG have opposing effects on growth and on activity of the iron-sulfur enzyme MiaB. *J. Bacteriol.* **2012**, *194* (2), 362–7.

(42) Hasnain, G.; Waller, J. C.; Alvarez, S.; Ravilious, G. E.; Jez, J. M.; Hanson, A. D. Mutational analysis of YgfZ, a folate-dependent

protein implicated in iron/sulphur cluster metabolism. *FEMS Microbiol. Lett.* **2012**, *326* (2), 168–72.

(43) Teplyakov, A.; Obmolova, G.; Sarikaya, E.; Pullalarevu, S.; Krajewski, W.; Galkin, A.; Howard, A. J.; Herzberg, O.; Gilliland, G. L. Crystal structure of the YgfZ protein from *Escherichia coli* suggests a folate-dependent regulatory role in one-carbon metabolism. *J. Bacteriol.* **2004**, *186* (21), 7134–40.

(44) Lee, H. H.; Kim, D. J.; Ahn, H. J.; Ha, J. Y.; Suh, S. W. Crystal structure of T-protein of the glycine cleavage system. Cofactor binding, insights into H-protein recognition, and molecular basis for understanding nonketotic hyperglycinemia. *J. Biol. Chem.* **2004**, *279* (48), 50514–23.

(45) Luka, Z.; Pakhomova, S.; Loukachevitch, L. V.; Newcomer, M. E.; Wagner, C. Folate in demethylation: the crystal structure of the rat dimethylglycine dehydrogenase complexed with tetrahydrofolate. *Biochem. Biophys. Res. Commun.* **2014**, *449* (4), 392–8.

(46) Gardner, P. R. Superoxide-driven aconitase Fe-S center cycling. *Biosci. Rep.* **1997**, *17* (1), 33–42.

(47) Tong, W. H.; Rouault, T. A. Metabolic regulation of citrate and iron by aconitases: role of iron-sulfur cluster biogenesis. *BioMetals* **2007**, *20* (3–4), 549–564.

(48) Chen, J. W.; Sun, C. M.; Sheng, W. L.; Wang, Y. C.; Syu, W. J. Expression Analysis of Up-Regulated Genes Responding to Plumbagin in *Escherichia coli*. *J. Bacteriol.* **2006**, *188* (2), 456–63.

(49) Chandramouli, K.; Unciuleac, M. C.; Naik, S.; Dean, D. R.; Huynh, B. H.; Johnson, M. K. Formation and properties of [4Fe-4S] clusters on the IscU scaffold protein. *Biochemistry* **2007**, *46* (23), 6804–6811.

(50) Mapolelo, D. T.; Zhang, B.; Naik, S. G.; Huynh, B. H.; Johnson, M. K. Spectroscopic and functional characterization of iron-sulfur cluster-bound forms of *Azotobacter vinelandii* (Nif)IscA. *Biochemistry* **2012**, *51* (41), 8071–8084.

(51) Andreini, C.; Rosato, A.; Banci, L. The relationship between environmental dioxygen and iron-sulfur proteins explored at the genome level. *PLoS One* **2017**, *12*, e0171279.

(52) Camponeschi, F.; Ciofi-Baffoni, S.; Banci, L. Anamorsin/Ndor1 Complex Reduces [2Fe-2S]-MitoNEET via a Transient Protein-Protein Interaction. *J. Am. Chem. Soc.* **2017**, *139*, 9479–9482.

(53) Golinelli-Cohen, M. P.; Lescop, E.; Mons, C.; Goncalves, S.; Clemancey, M.; Santolini, J.; Guittet, E.; Blondin, G.; Latour, J. M.; Bouton, C. Redox Control of the Human Iron-Sulfur Repair Protein MitoNEET Activity via Its Iron-Sulfur Cluster. *J. Biol. Chem.* **2016**, *291* (14), 7583–7593.

(54) Ferecatu, I.; Goncalves, S.; Golinelli-Cohen, M. P.; Clemancey, M.; Martelli, A.; Riquier, S.; Guittet, E.; Latour, J. M.; Puccio, H.; Drapier, J. C.; Lescop, E.; Bouton, C. The diabetes drug target MitoNEET governs a novel trafficking pathway to rebuild an Fe-S cluster into cytosolic aconitase/iron regulatory protein 1. *J. Biol. Chem.* **2014**, *289* (41), 28070–28086.